HZ BOOKS
华章教育

Pearson

经典原版书库

增强现实

原理与实践

[奥] 迪特尔·施马尔斯蒂格（Dieter Schmalstieg）
[美] 托比亚斯·霍勒尔（Tobias Höllerer） 著

（英文版）

Augmented Reality
Principles and Practice

PRINCIPLES AND PRACTICE

Augmented REALITY

Dieter SCHMALSTIEG
Tobias HÖLLERER

机械工业出版社
China Machine Press

经典原版书库

增强现实
原理与实践
（英文版）

Augmented Reality
Principles and Practice

[奥] 迪特尔·施马尔斯蒂格（Dieter Schmalstieg）
[美] 托比亚斯·霍勒尔（Tobias Höllerer） 著

机械工业出版社
China Machine Press

图书在版编目（CIP）数据

增强现实：原理与实践（英文版）/（奥）迪特尔·施马尔斯蒂格（Dieter Schmalstieg）等著．—北京：机械工业出版社，2018.5
（经典原版书库）
书名原文：Augmented Reality：Principles and Practice

ISBN 978-7-111-59910-4

Ⅰ.增…　Ⅱ.迪…　Ⅲ.虚拟现实－英文　Ⅳ.TP391.98

中国版本图书馆 CIP 数据核字（2018）第 091758 号

本书版权登记号：图字　01-2016-8660

出版发行：机械工业出版社（北京市西城区百万庄大街 22 号　邮政编码：100037）

责任编辑：曲　熠	责任校对：殷　虹
印　　刷：中国电影出版社印刷厂	版　　次：2018 年 6 月第 1 版第 1 次印刷
开　　本：186mm × 240mm　1/16	印　　张：32.25（含 1 印张彩插）
书　　号：ISBN 978-7-111-59910-4	定　　价：99.00 元

凡购本书，如有缺页、倒页、脱页，由本社发行部调换
客服热线：（010）88378991　88361066　　投稿热线：（010）88379604
购书热线：（010）68326294　88379649　68995259　　读者信箱：hzjsj@hzbook.com

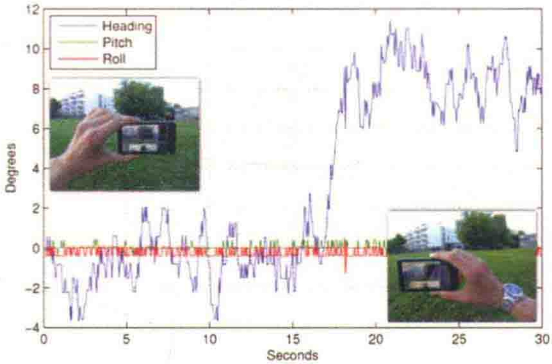

Figure 3.11 Every modern smartphone contains a magnetometer, but precision of that sensor alone is often very poor. The image shows the heading error over time as a metallic watch worn on the user's right hand comes close to the device. Courtesy of Gerhard Schall.

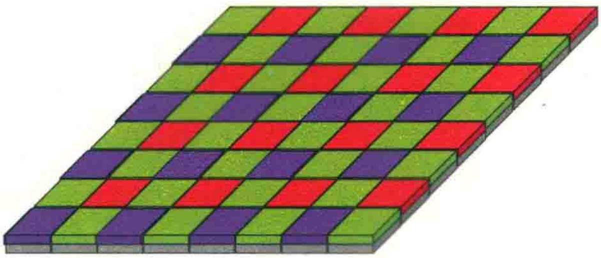

Figure 3.16 Modern digital cameras use CCD sensors to determine the intensity of incoming light. Color is added by using a filter grip with a Bayer pattern.

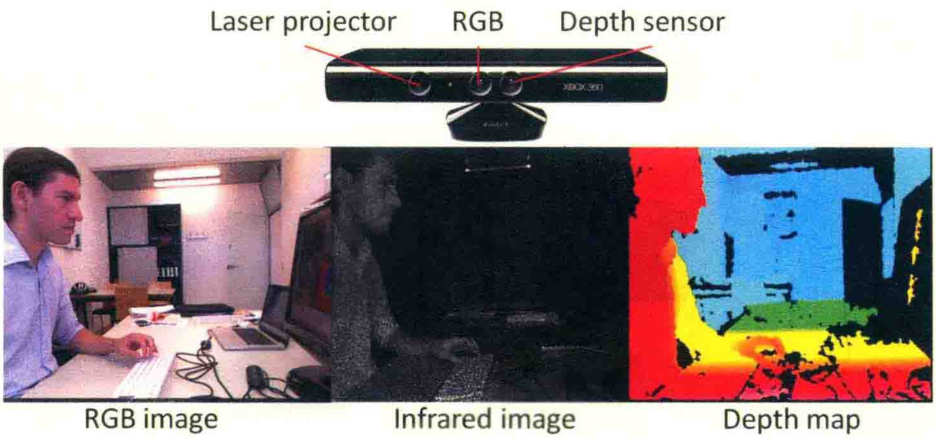

Figure 3.18 (top) The Microsoft Kinect V1 is an RGB-D camera intended for controlling XBox games using gesture recognition. (bottom left) Its RGB camera delivers a conventional color image. (bottom middle) A laser projector casts an invisible infrared dot pattern on the scene. (bottom right) The depth sensor uses an infrared camera to observe the dot pattern and computes a depth map from it. Here the depth map is shown with color coding from red = near to blue = far.

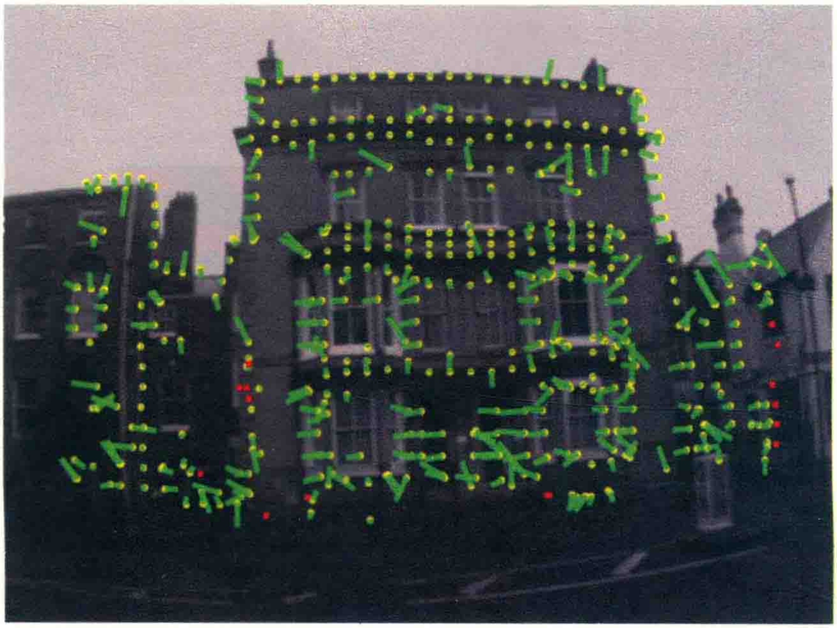

Figure 3.23 The Going Out system from Cambridge University tracks samples along strong edges in the image and compares them to a known model of the outdoor scene. Courtesy of Gerhard Reitmayr and Tom Drummond.

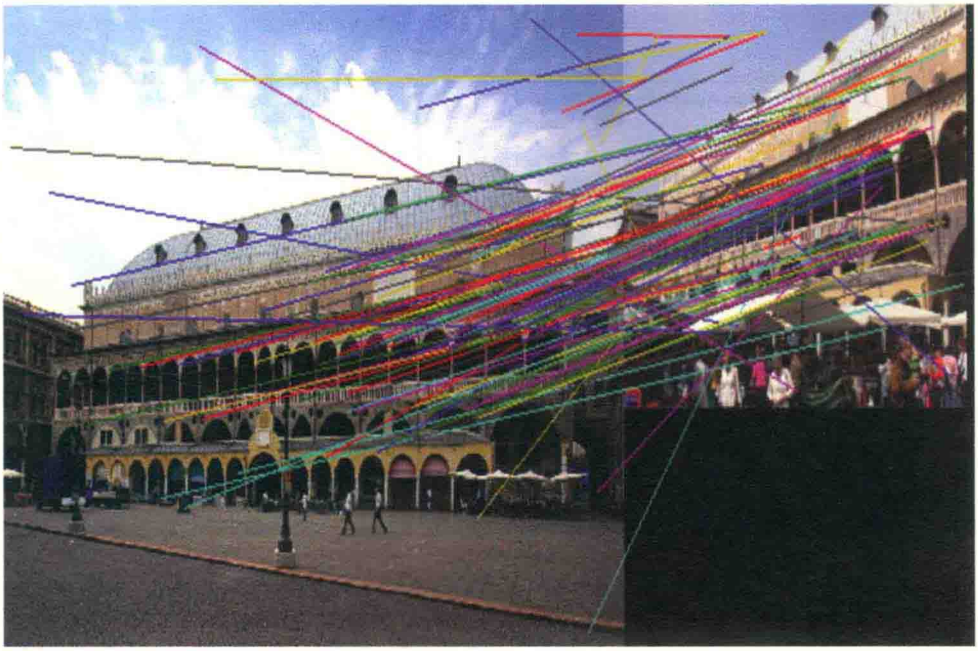

Figure 3.26 Feature matching allows the system to identify known interest points from a tracking model in a new view of the scene. From a sufficient number of correct point associations, a scene can be identified and the current camera pose can be determined. Courtesy of Martin Hirzer.

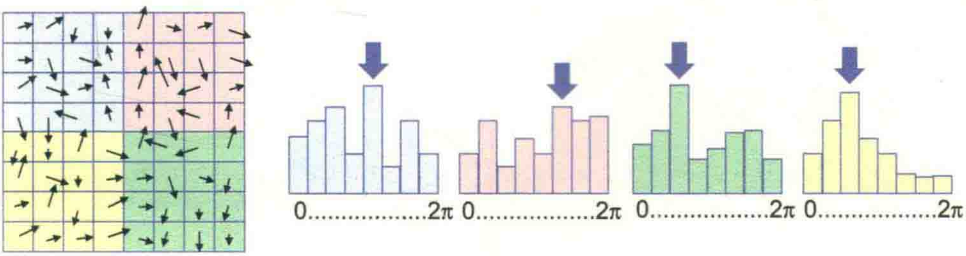

Figure 4.11 SIFT determines gradient vectors for every pixel of the (here: 8×8) image patch (left). A (here: 2×2) descriptor array with (here: 8-bin) histograms relating cumulative gradient vector magnitude to gradient orientation is built (right). In this example, the descriptor has $2 \times 2 \times 8 = 32$ dimensions.

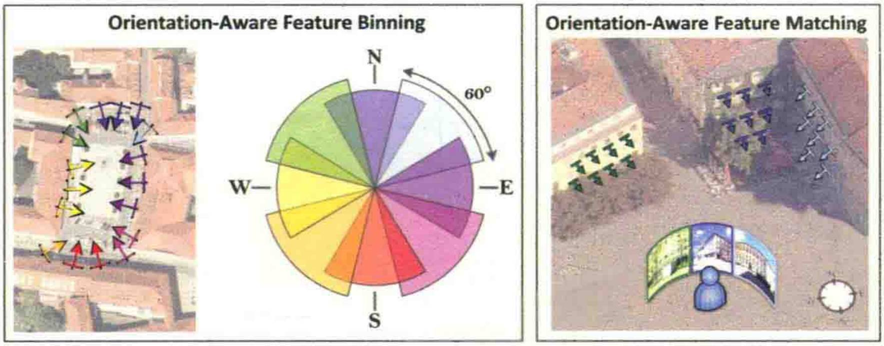

Figure 4.27 A magnetometer (compass) can be used as a source of prior information to narrow the search for point correspondences to those with a normal facing approximately toward the user. Courtesy of Clemens Arth.

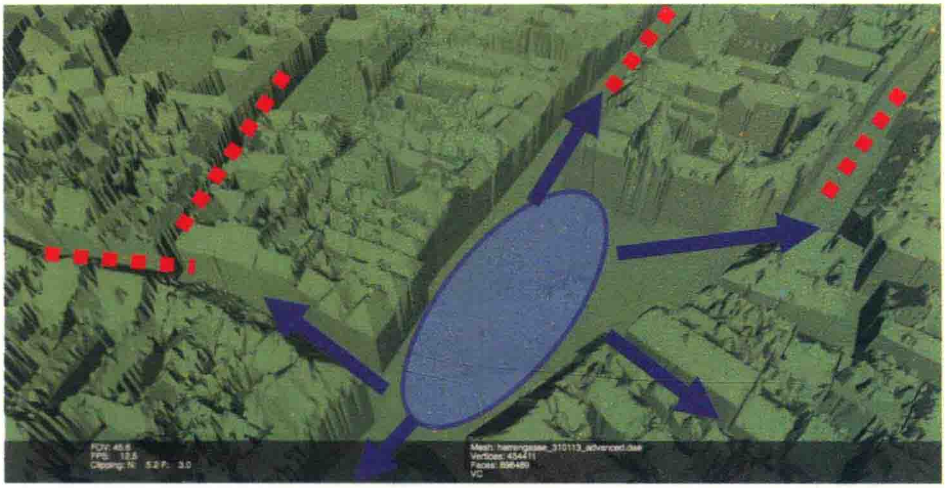

Figure 4.29 The potentially visible set for the central square contains the street segments immediately connected to the square (blue arrows), but not the street segments after one or more turns (dashed red lines).

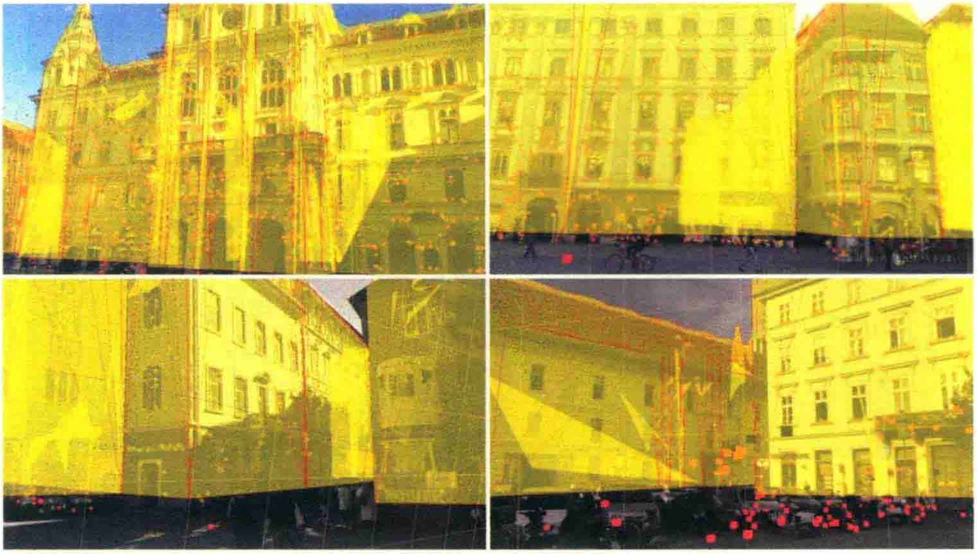

Figure 4.34 Multiple images from a sequence tracked with 6DOF SLAM on a client, while a localization server provides the global pose used to overlay the building outlines with transparent yellow structures. Courtesy of Jonathan Ventura and Clemens Arth.

Figure 4.35 This SLAM sequence starts with tracking a facade (overlaid in yellow), for which a global pose has been determined by a server. The images in the bottom row cannot continue tracking with information known to the server; the poster in the foreground, which has been incorporated into the SLAM map, is used for tracking instead. Courtesy of Jonathan Ventura and Clemens Arth.

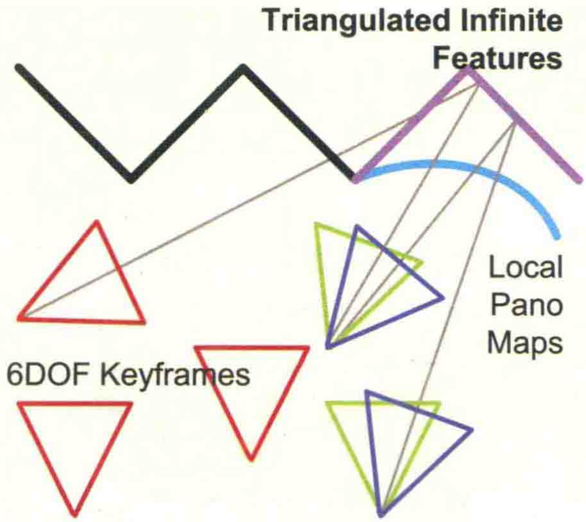

Figure 4.36 A SLAM system that can handle both general 6DOF motion and pure rotation has the advantage that the user is not constrained to a certain type of motion. It also presents the opportunity to recover 3D features (magenta) from panoramic features (cyan) when additional views become available. Courtesy of Christian Pirchheim.

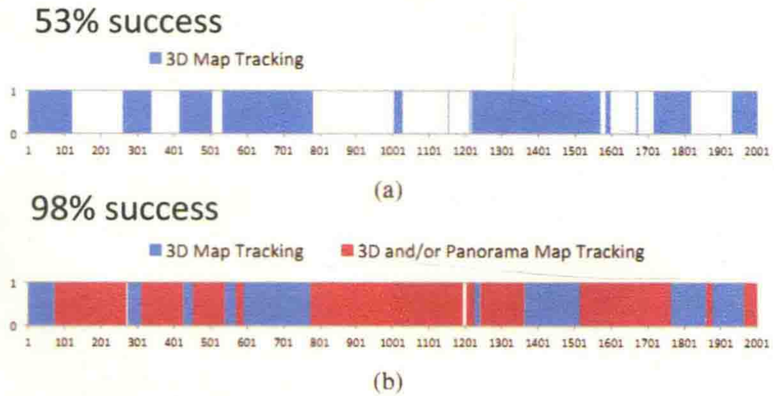

Figure 4.37 The combination of 6DOF and panoramic SLAM delivers much more robust tracking performance during arbitrary user motion. (a) Conventional 6DOF SLAM can track the pose for only 53% of the frames. (b) Combined SLAM can track the pose in 98% of the frames. Courtesy of Christian Pirchheim.

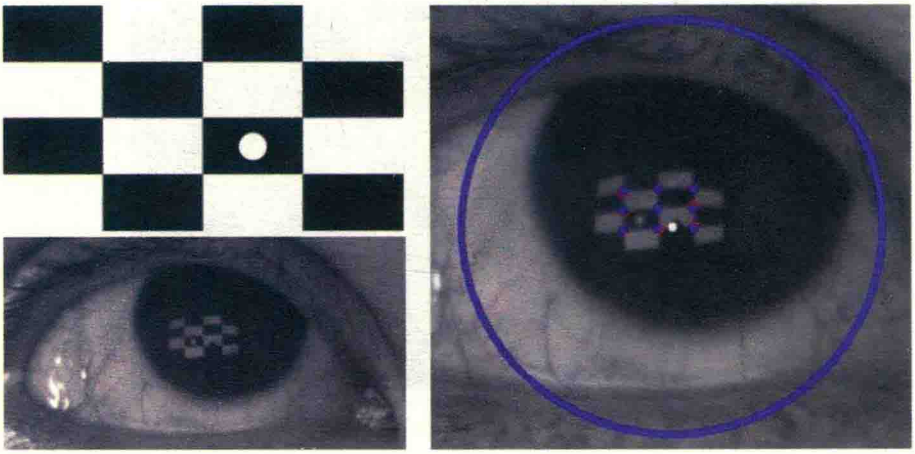

Figure 5.6 An inward-facing camera mounted in an HMD can be used to detect a projected checkerboard pattern and derive the eye's position and orientation relative to the display. Courtesy of Alexander Plopski.

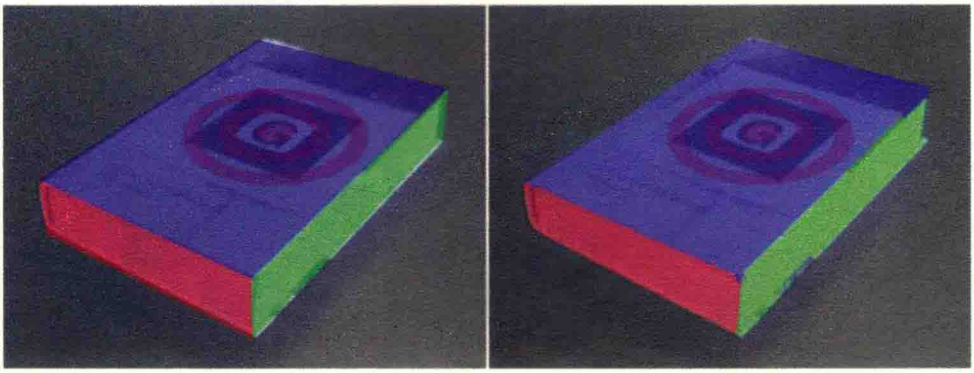

Figure 6.6 By searching near the projected edge of a phantom object for the true edge of the corresponding real objects (left), occlusion boundaries can be corrected (right). Courtesy of Stephen DiVerdi.

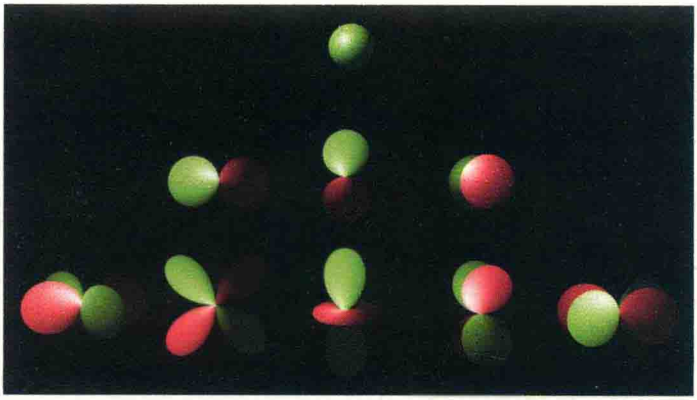

Figure 6.16 Spherical harmonics are basis functions defined over a spherical domain. The three rows show the spherical harmonics for bands 0, 1, and 2.

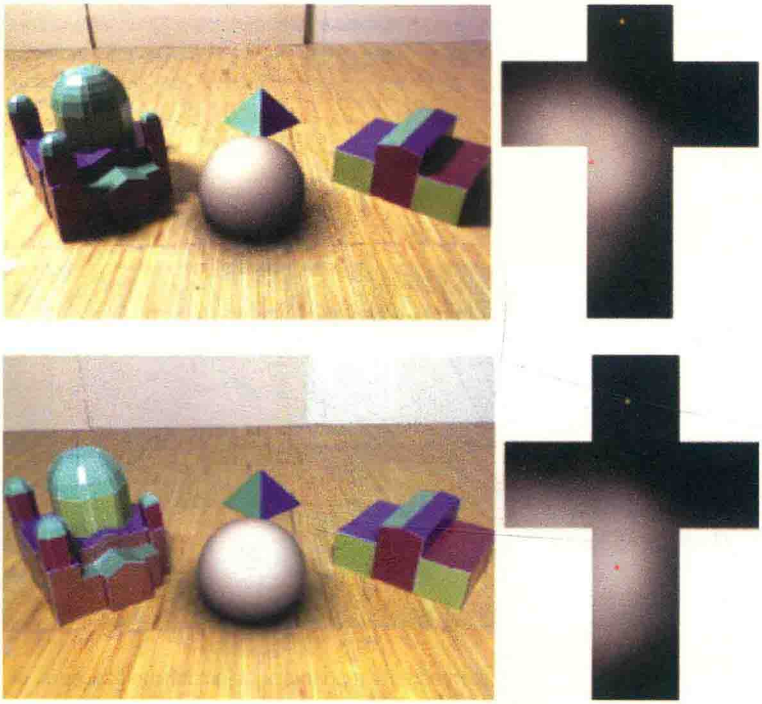

Figure 6.17 Directional light can be estimated from diffuse objects, such as the church model, and applied to a virtual object, such as the white ball. The right column shows the estimated incident light as a cube map. Note how the change of the strongest lighting direction, indicated by the red dot in the environment map, corresponds to the movement of the white highlight on the dome. Courtesy of Lukas Gruber.

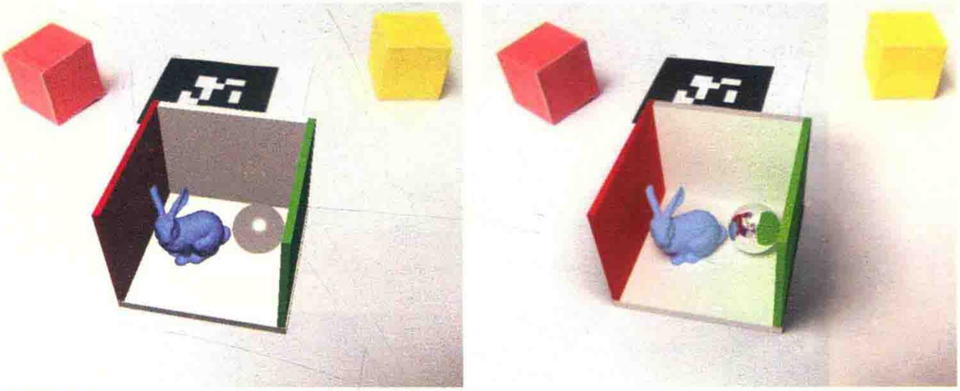

Figure 6.21 Real-time path tracing enables realistic global illumination effects, as demonstrated in this comparison of local (left) and global (right) illumination rendering for augmented reality. Courtesy of Peter Kán.

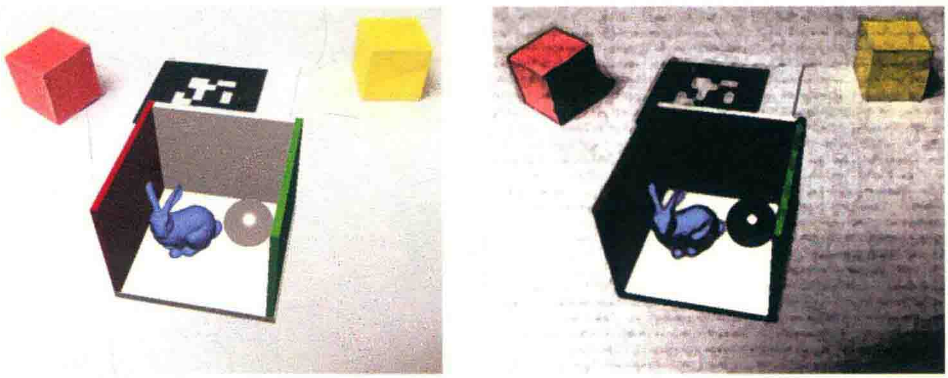

Figure 6.30 Stylized AR can be used for artistic impression, where the real and virtual parts of the scene assume the same style. Original scene image courtesy of Peter Kán.

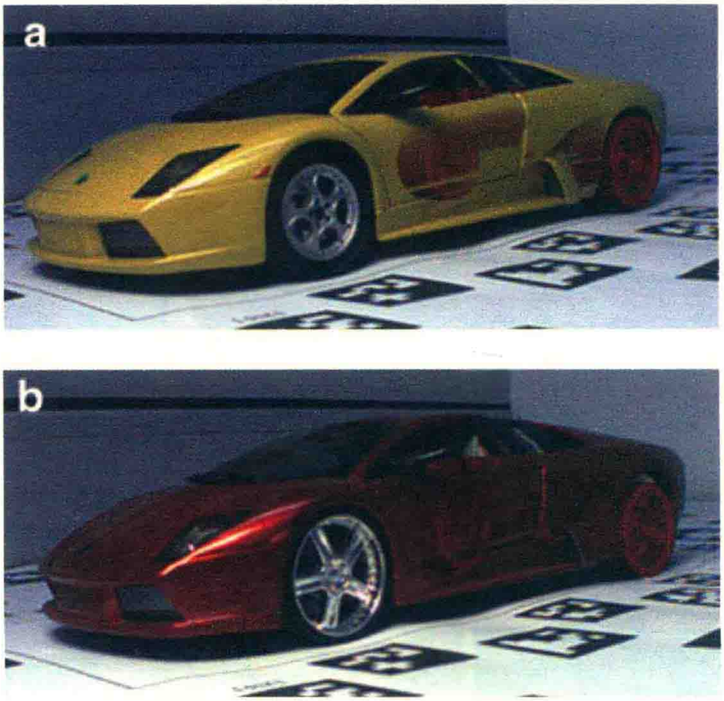

Figure 7.6 (top) The visualization clearly shows the internals of the car in the rear. (bottom) A poor choice of color severely impacts the perception of the occluded visualization. Courtesy of Denis Kalkofen.

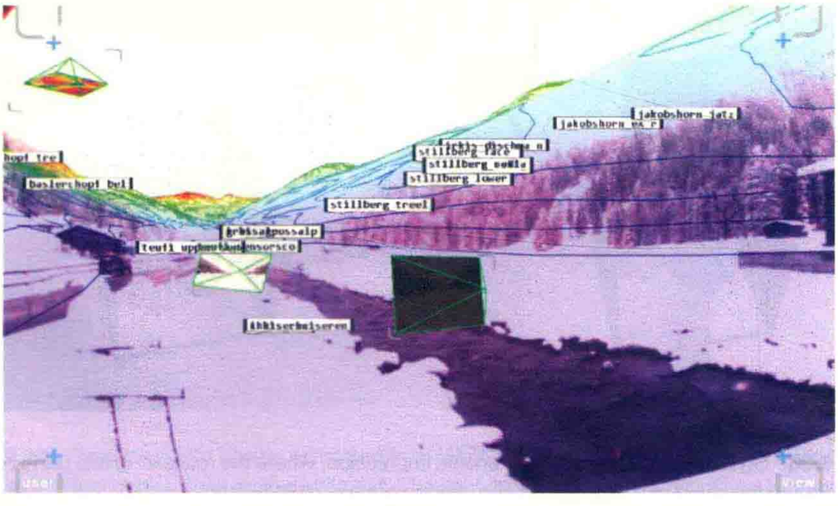

Figure 7.7 Hydrosys displays locations of stations in a global sensor network as well as interpolated temperature plotted as geodesic contours. Courtesy of Eduardo Veas and Ernst Kruijff.

Figure 7.13 In this example, the body of a real car is the occluder for a virtual engine. After extracting contours as important shape hints, a 2D distance transform is applied to make the occluder seem more solid. Courtesy of Denis Kalkofen.

Figure 8.14 Turning an ordinary surface into a touchscreen with a projector–camera system. Courtesy of Claudio Pinhanez (copyright IBM 2001).

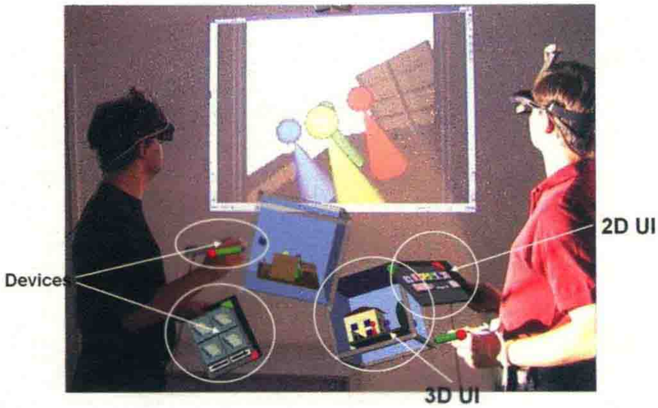

Figure 8.29 Concurrent first-person view seen on the wall projection, and third-person view seen through a head-mounted display. Courtesy of Gerd Hesina and Anton Fuhrmann.

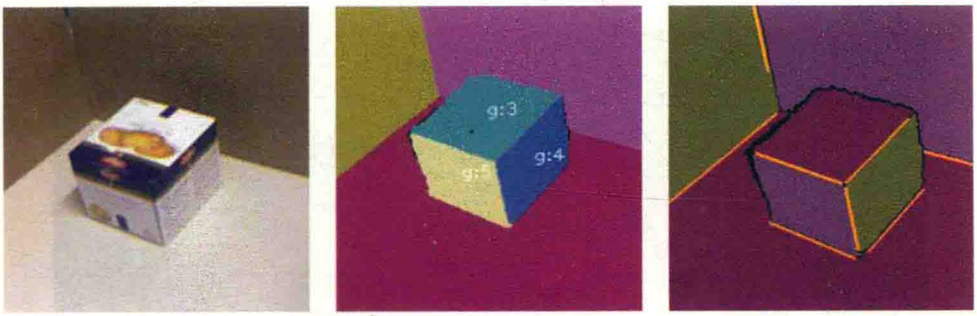

Figure 9.11 (left) View of a simple scene from an RGBD sensor. (middle) Planes segmented from the depth image. (right) Geometric scene understanding detects straight edges, shown as yellow lines, and parallel planes, shown in the same color. Courtesy of Thanh Nguyen.

Figure 11.1 The Signpost system lets an outdoor AR user follow a route consisting of waypoints (red cylinders). Courtesy of Gerhard Reitmayr.

Figure 11.2 The Indoor Signpost system highlights the next doorway along a path and shows a 3D arrow pointing in the direction of the final destination. Courtesy of Daniel Wagner.

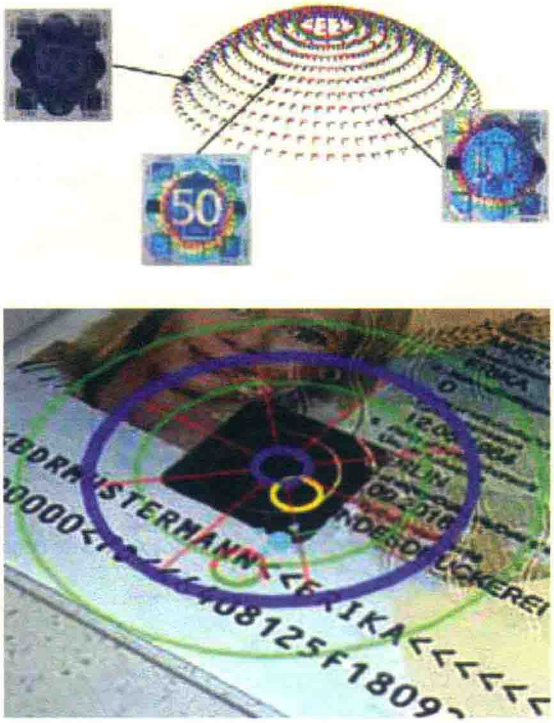

Figure 11.8 (top) The appearance of a hologram varies with the incident viewing direction. (bottom) The yellow circle directs the user toward a specific viewing direction, encoded as the angle and distance to the center of the pie slice visualization. Courtesy of Andreas Hartl.

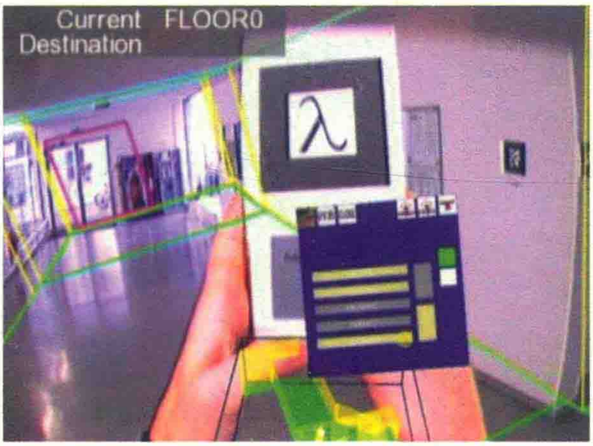

Figure 11.12 A world-in-miniature can be attached to a handheld or arm-mounted prop. Courtesy of Gerhard Reitmayr.